Metrol. Meas. Syst., Vol. 27 (2020) No. 4, pp. 589–599
DOI: 10.24425/mms.2020.134840

METROLOGY AND MEASUREMENT SYSTEMS
Index 330930, ISSN 0860-8229
www.metrology.wat.edu.pl

MACHINE VISION DETECTION OF POINTER FEATURES IN IMAGES OF ANALOG METER DISPLAYS

Hai-Bo Zhuo[1)], Fu-Zhong Bai[1,2)], Yong-Xiang Xu[1,2)]

1) *Inner Mongolia University of Technology, College of Mechanical Engineering, Huhhot 010051, China* (*278813017@qq.com*, ✉ *fzbaiim@163.com*, +86 0471 6575 472, *nmxyx_63@163.com*)
2) *Inner Mongolia Key Laboratory of Special Service Intelligent Robotics, Huhhot 010051, China*

Abstract

In automatic and accurate reading recognition of analog meters based on machine vision, one of important issues is the detection of pointer features, which includes the meter center and pointer image processing. The current automatic-recognition approaches to reading analog meters often consist in locating the meter center based on the dial region or its border. The located center is not coincident with the rotation center of pointer which leads to inevitable reading errors. In the paper, the centripetalism of annular scale lines is used to calculate the position of the pointer rotation center. First, it uses the region growing method to locate the dial region and uses the eccentricity measure to extract annular scale lines. Second, the parameters of these scale lines are estimated with the Hough transform method. Then, the common intersection of a group of lines, i.e., the meter rotation center, is determined with the maximum probability criterion. Finally, the pointer centerline and direction are detected through the calculated center and the Hough transform results. The simulated and experimental results demonstrate that the proposed method can accurately locate the pointer rotation center and obtain pointer centerline. Moreover, it is applicable to the meter image captured under a slant camera view or with uneven light illumination.

Keywords: pointer meter, pointer rotation center, annular scale lines, pointer features.

1. Introduction

The pointer meter is widely used in industrial fields and power transmission systems due to its simple structure, strong resistance to electromagnetic interference and low cost. In the process of regular calibration or metrological verification, the operator has to manually record the indicated value. This manual technique is inconvenient and inefficient, and the reliability and accuracy of reading are relatively low [1, 2]. Also, the non-digital signal output of the pointer meter cannot be processed by a computer. Therefore, an automatic reading method that transforms the value into the digital signal [3, 4] should be urgently worked out for wider application. In recent years, some automatic pointer meter recognition methods have been developed [5, 6] which can be summarized into two categories. First, the template matching-based method is used to determine

the angle between the zero-scale line and the pointer centerline and then the indicated value is obtained [7]. Second, the distance method is used to obtain the indicated value by comparing the pointer centerline with scale lines [8–10].

In the case of automatic reading methods for pointer meters, determining the meter center location is an essential task that can ensure the accuracy of pointer extraction and reading value. In general, the circular shape feature of the meter dial is used to locate the meter center. For example, Chi *et al.* [11] use the region growing method to segment the dial region. Then the central point of external rectangle of dial region is used as the meter center. Ma *et al*. [12] use the roundness feature of connected regions to extract the small light-colored region around the center of the meter. Then the meter center is estimated by the gravity center method.

The above-mentioned region based methods are easily affected by illumination shadows, shape defects or surface contamination. At the same time, only front viewing meter image can be processed. If the image of meter taken by a camera is not front viewing, spatial deformation will occur due to the perspective transformation of camera. The circular meter dial will become ellipsoidal. And the application of these methods the deformed circle shape will yield an inaccurate location of the center as it no longer coincides with the meter center. In result, the final reading may have large deviation.

It is well known that the extended lines of annular scale lines evenly distributed on the dial border will pass through the rotation center of pointer. This paper bases on the application of the centripetalism principle of annular scale lines to locate the rotation center of pointer. In this approach, the dial region is segmented by, first, using the region growing method. Then, the linear objects are extracted by applying the eccentricity measure to binary images. Next, the Hough transform is employed to estimate the fitting parameters of scale lines. The pointer rotation center location is obtained through determining a common intersection point of the detected lines. Finally, based on the located center, the pointer centerline and its direction are detected.

The principle of the proposed method is introduced with the help of a simulation example. Further, the experiments with two different pointer meters are presented and the performances of two methods are compared. Experiments with pointer detection based on different methods are then conducted and the results are compared.

2. Principle of method

2.1. Dial region segmentation

The region-growing method is adopted to extract the dial region from the meter image. The main steps are as follows.

1. Since the dial is usually white, the region with a high gray level or the pixel point with the highest gray level in the meter is selected as the growing seed point [13].
2. Taking advantage of the similarity of the region's gray level, the expansion of the dial region is conducted from the seed point. If the difference of gray value between the seed and the pixels surrounding the seed is less than a given threshold value, these pixels will be combined with seed point into the same region. New pixels will be taken as a new seed points to continue the above process until no pixels meet the requirement.

The gray level of the dial region is obviously different from that of the meter border, so a nearly circular dial region can be segmented. The pointer meter image is then processed and the resulting segmented dial image is shown in Fig. 1.

Metrol. Meas. Syst., Vol. 27 (2020), No. 4, pp. 589–599
DOI: 10.24425/mms.2020.134840

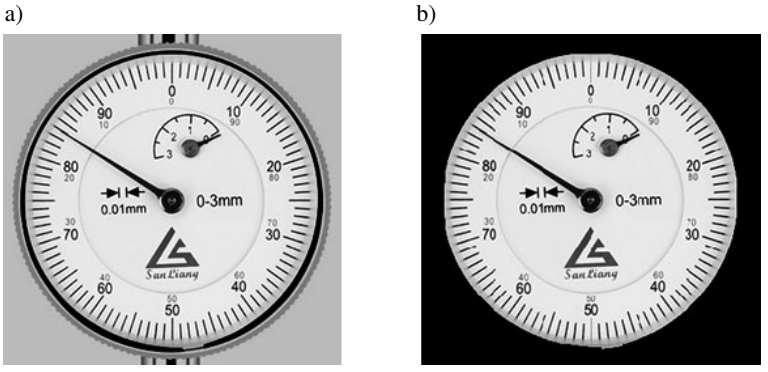

Fig. 1. Results of dial segmentation of the pointer meter: a) meter image, b) dial region.

2.2. Extraction of linear objects

In the binary dial image, one can use the eccentricity measure to extract linear objects such as scale lines and the pointer. For the linear objects of different direction and size, the eccentricity of ellipse [14, 15] can more accurately describe their shape characteristics compared with circular or rectangular features. The eccentricity of a connected region is given by

$$e = \sqrt{1 - b^2/a^2}\,. \tag{1}$$

In the expression above, a^2 and b^2 are calculated according to the following equations,

$$a^2 = 8\left[M_{xx} + M_{yy} + \sqrt{\left(M_{xx} - M_{yy}\right)^2 + 4M_{xy}^2}\right], \tag{2}$$

$$b^2 = 8\left[M_{xx} + M_{yy} - \sqrt{\left(M_{xx} - M_{yy}\right)^2 + 4M_{xy}^2}\right], \tag{3}$$

where M_{xx}, M_{yy} and M_{xy} are the second-order central moments of a connected region in binary images, and they are calculated according to the following equations,

$$M_{xx} = \frac{1}{N}\sum_{i=1}^{N}(x_i - X_0)^2, \tag{4}$$

$$M_{yy} = \frac{1}{N}\sum_{i=1}^{N}(y_i - Y_0)^2, \tag{5}$$

$$M_{xy} = \frac{1}{N}\sum_{i=1}^{N}(y_i - Y_0)(x_i - X_0), \tag{6}$$

where (X_0, Y_0) are the center coordinates of region, x_i and y_i are horizontal and vertical coordinates of the pixels in the region, and N is the pixel number of the region. If this region is near to a circle, then the eccentricity is close to 0. If this region is close to a linear shape, then the eccentricity is close to 1. Therefore, the eccentricity measure can distinguish the linear objects with other shapes.

The binary dial image which is shown in Fig. 2a can be obtained from the segmented dial image with Otsu's algorithm [16]. In this figure, the object regions are expressed as white pixels. The eccentricity values of all connected components are calculated and their histogram figure is shown in Fig. 2b. A threshold value close to 1 is then selected. For example, we selected 0.97 for this paper, and then we were able extract the annular scale lines that are shown in Fig. 2c.

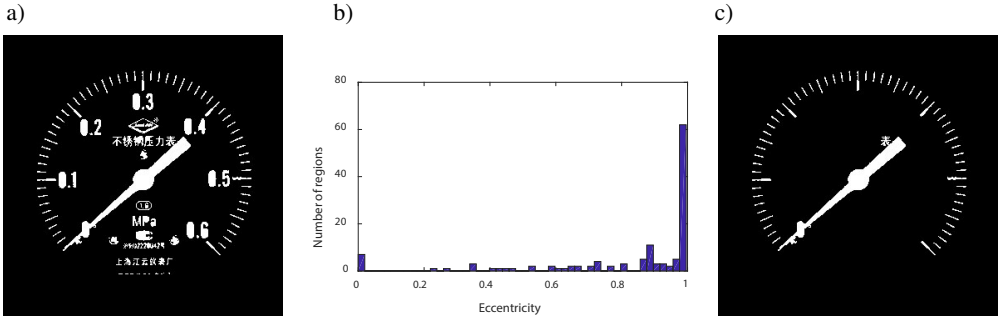

Fig. 2. Extraction of linear objects with the eccentricity measure: a) binary dial image, b) eccentricity histogram of connected regions in binary dial image, c) extracted linear objects.

2.3. Location of the rotation center of the pointer

In general, the annular scale lines in an analog meter are evenly distributed on the dial border and, when extended, the lines pass through the rotation center of the pointer. If the fitting lines for them are obtained, the rotation center can be located. Here we use the popular *Hough transform method* (HTM) to detect the parameters of linear objects.

Based on the principle of HTM, a point of interest (x_i, y_i) in the image space will map to a sinusoidal curve in the Hough space defined by ρ and θ according to the following equation.

$$\rho = x_i \cos\theta + y_i \sin\theta, \tag{7}$$

where ρ represents the normal distance from the origin to this point, and θ represents the angle of the normal vector with the horizontal axis. The step angle of θ can be set to 0.1 degree and its possible range is from –90 to 90 degrees. A group of points located in a line will correspond to a series of sinusoidal curves with a common intersection point (θ_i, ρ_i) in the Hough space [17–19]. Therefore, by using the HTM we can obtain the parameters of lines and then the fitting line in image space can be written as

$$y = \left(\tan^{-1}\theta_i\right) x + \left(\sin^{-1}\theta_i\right) \rho_i \,. \tag{8}$$

In addition, the HTM can avoid the noise effect and line discontinuity to a large extent. In this case, we can fit all linear objects in the spatial image among which the pointer is included. To obtain the sharp peak and ensure the uniqueness of the result, the object image as shown in Fig. 2c is thinned before the Hough transform, and the result of the thinning is shown in Fig. 3a. Then the Hough transform is performed, and the result is shown in Fig. 3b.

After the parameters of all fitting lines are calculated, we can determine the rotation center coordinates with the maximum probability criterion. The main steps of center location algorithm includes are as follows. (1) A two-dimensional array with zero as initial value is built as an accumulator as shown in Fig. 4, where each grid represents a pixel corresponding to meter image.

Metrol. Meas. Syst., Vol. 27 (2020), No. 4, pp. 589–599
DOI: 10.24425/mms.2020.134840

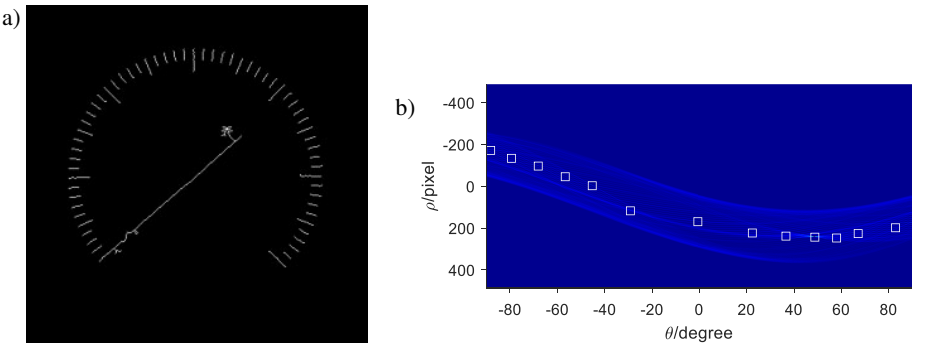

Fig. 3. Results of the thinning and the application of the Hough transform to the object image as shown in Fig. 2c, a) thinning, b) Hough transform.

(2) One is added to the value of the grid that the fitting line passes through. (3) After all fitting lines are plotted, the position corresponding to the maximal value in the array can be found and the rotation center is determined. If there are two or more maxima in the array, the following formula is used to determine the coordinate of rotation center.

$$\begin{cases} x_0 = \dfrac{1}{n}\displaystyle\sum_{i=1}^{n} x_i', \\ y_0 = \dfrac{1}{n}\displaystyle\sum_{i=1}^{n} y_i', \end{cases} \tag{9}$$

where (x_0, y_0) are the coordinates of the rotation center, (x_i', y_i') are the positions corresponding to the maximal value, and n is the number of points.

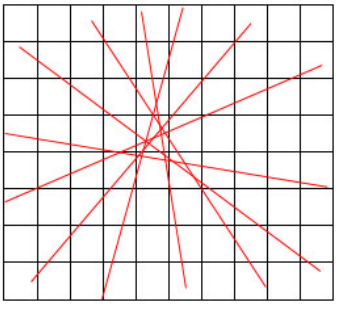

Fig. 4. Diagram of a 2D accumulator used in the determination of the rotation center.

2.4. Detection of pointer and its direction

The pointer is the longest connected component in the dial image, and so it will correspond to the maximum peak point in the Hough space. Therefore, we can obtain the pointer centerline by finding out the coordinate (θ_M, ρ_M) of this maximum peak. In order to avoid the problem of the pointer centerline not passing through the rotation center of pointer, the center (x_0, y_0) calculated

in Section 2.3 is taken as another constraint in the detection of the pointer. The equation of pointer centerline is given by

$$y - y_0 = \left(\tan^{-1}\theta_{\mathrm{M}}\right)(x - x_0)\,. \tag{10}$$

After the pointer is detected, the pointer direction also should be determined. In the extraction results for the annular scale lines and the pointer as shown in Fig. 2c, the largest connected component including the rotation center must be the pointer region. Then the pointer direction is determined through comparing the relative position between the gravity center of the pointer region and the rotation center.

3. Theoretical analysis of the method performance

1. Feasibility verification of the method. An image that includes annular scale lines is simulated with short lines evenly distributed around the circle border. The center of the circle, namely, the intersection point of all short lines, is (141, 141) pixel. With the HTM, the detection results are shown in Fig. 5 and the detected center is the same as the given value. Also, the detected lines highly agree with the original lines. The simulated results show that the rotation center can be located on the basis of these short annular scale lines. Furthermore, the method based on structural features is also more reliable which can be concluded from the following experiment.

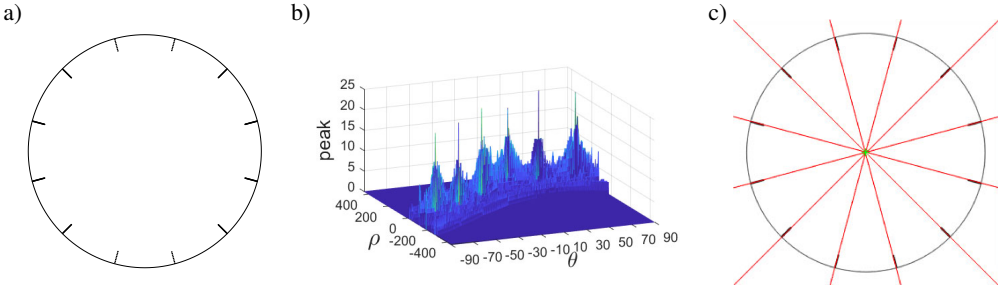

Fig. 5. Example of center location for simulated meter image: a) ideal image with simulated annular scale lines, b) Hough transform result of simulated image, c) center location results.

2. Performance of the method applied for the non-front viewing image. When we recognize the reading value of pointer meter with the naked eye, the eye sight should be perpendicular to the meter surface. There is a similarity between human vision and machine vision, and so the camera captured image also should poses in the front viewing.

However, it is very difficult to adjust the optical axis of a camera perpendicular to the meter surface. The captured image has often slight spatial deformation due to the perspective transformation of camera. The circular meter dial will become ellipsoid and the ellipse's center will no longer coincide with the center of the circular dial. This problem is illustrated in Fig. 6. A front viewing image with extended annular scale lines and circular border is shown in Fig. 6a and its right viewing image is shown in Fig. 6b which is similar to the image captured by the camera from the right side. The dial center calculated with the traditional method is same as it comes to the center of the ellipse after deformation, *i.e.*, the central point of the external rectangle of the ellipse region. However, in Fig. 6c we can see obviously that it has large deviation from the rotation center.

Metrol. Meas. Syst., Vol. 27 (2020), No. 4, pp. 589–599
DOI: 10.24425/mms.2020.134840

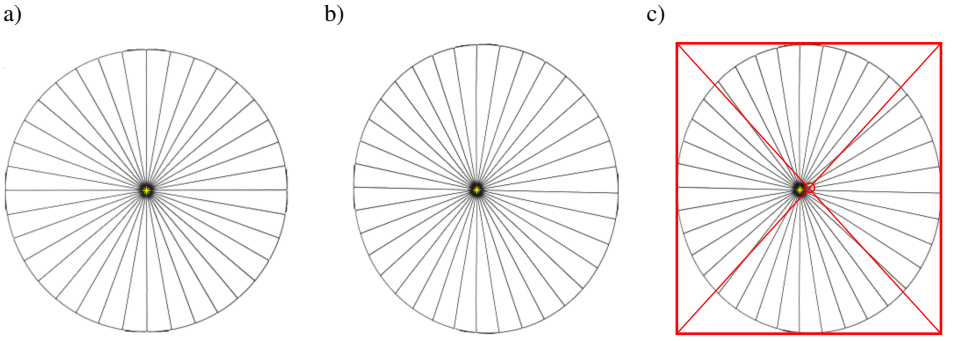

Fig. 6. Illustration of spatial deformation. (a) and (b) describe the image captured in front and right views, (c) the difference of rotation center (the symbol'*' in the three figures) and ellipse's center expressed as 'o' in Figure (c).

Therefore, traditional region-based methods no longer prove accurate when applied to the non-front viewing image. But it should be noted here that the annular scale lines in the deformed image will still coincide with the rotation center of the pointer.

4. Experiments

Two types of pointer meters are tested in the experiments. One meter is a dial pointer meter, in which annular scale lines are distributed equally in whole circular border. The other is a pressure gauge with only a part of annular scale lines and many words appearing on the meter dial. In addition, the camera view and light illumination are also considered in the experiment.

The first set of experiments is conducted with a dial pointer meter and its images captured under different camera views are shown in Figs. 7a and 7d. With the proposed method almost all

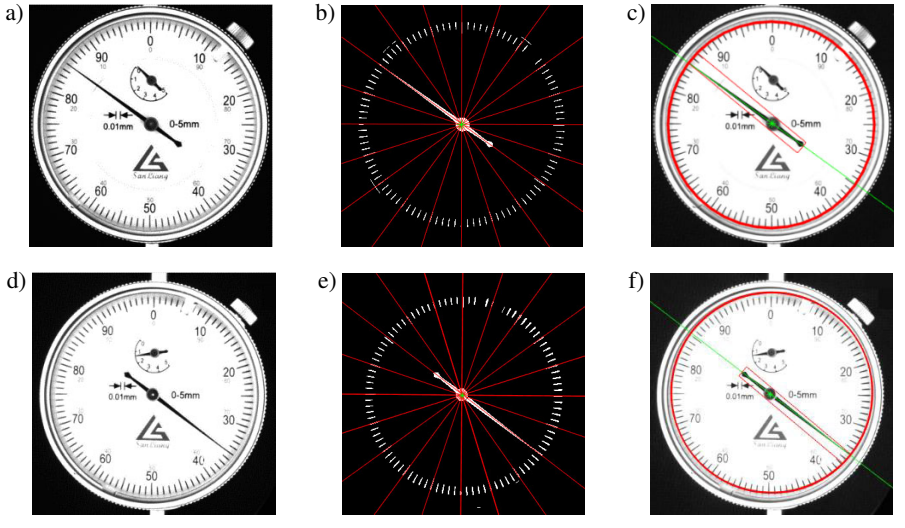

Fig. 7. Pointer features detection of an analog dial meter under different camera views: a) and d) original meter images, b) and e) annular scale lines and corresponding fitting lines, c) and f) the pointer and its rotation center.

annular scale lines as well as the pointer are extracted in both images. The fitting straight lines for the longer scale lines are plotted in Figs. 7b and 7e. The detected pointer and its centerlines are shown in Figs. 7c and 7f.

Based on the determined center and the minimum distance from the center to the dial edge as the radius value, we plot a standard circle in the original meter image. By comparing of the dial border with the standard circle, it can be found that the slight spatial deformation is included in the image as shown in Fig. 7d. This indicates that it is captured under a small slant viewing angle.

The second set of experiments is conducted with a pressure gauge. At first, the images captured under a slant camera view are considered which are shown in Figs. 8a and 8d. This can also be found by comparing the standard circle plotted in Figs. 8c and 8f with the dial border. In another image shown in Fig. 8g, uneven light illumination is included and so only a small number of lines can be extracted. Three images are processed in steps similar to the experiment above.

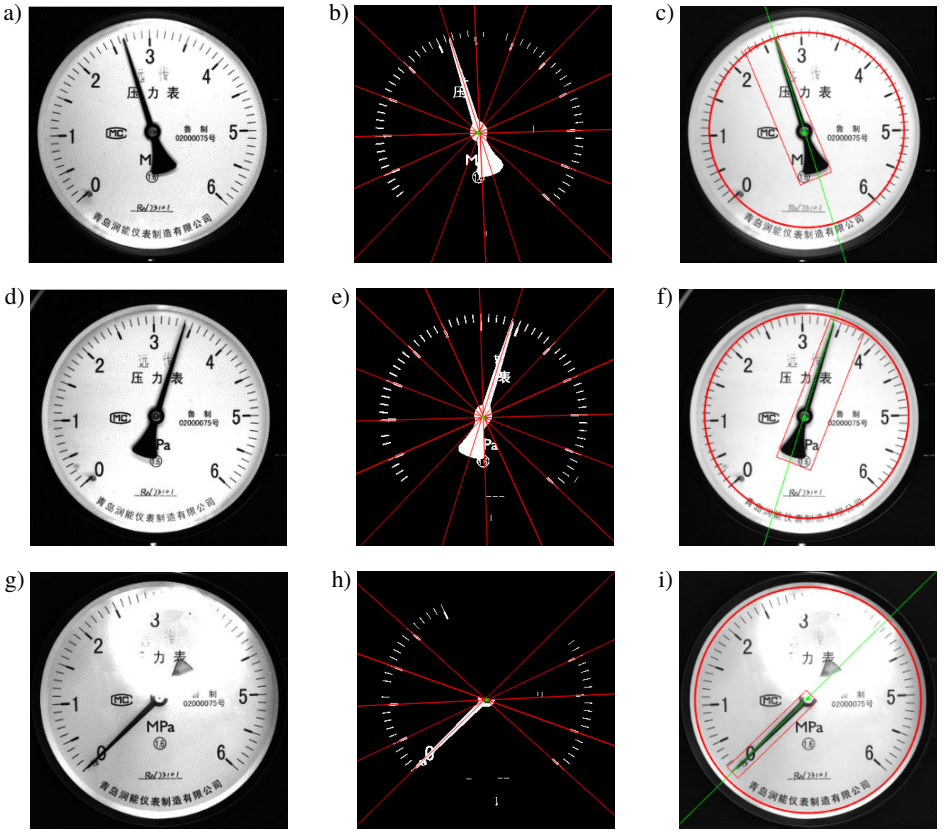

Fig. 8. Pointer features detection of a pressure gauge under different camera views and uneven light illumination. Original images (first column), annular scale lines and corresponding fitting lines (second column) and the pointer and its rotation center (last column).

By using the algorithm of [11] and our method, the pointer rotation centers of five images are obtained and listed in Table 1. Then the manually-measured values are employed as true values. The absolute error is defined as the distance between the located value and the manually-measured value. The detected results indicate that our method is good at detecting the pointer features and

is superior to the algorithm of [11] with respect to accuracy and robustness of center location. It also should be noted that the image in Fig. 8g posed a particular challenge in the detection of the pointer rotation center because only a limited number of scale lines can be used. However, our method can still detect reliably and has minor absolute errors.

Table 1. Comparison of rotation center of pointers (unit: pixel).

Figure number	Manual measured values	Algorithm of [11]		Our method	
		Located dial result	Absolute error	Located rotation center	Absolute error
Fig. 6a	(182, 181)	(183, 181)	1	(182, 181)	0
Fig. 6d	(182, 184)	(181, 185)	1.41	(182, 185)	1
Fig. 7a	(177, 179)	(177, 182)	3	(177, 181)	1.41
Fig. 7d	(168, 168)	(167, 172)	2.24	(168, 169)	1
Fig. 7g	(194, 182)	(191, 184)	3.6	(194, 183)	1

Although the absolute error in Table 1 is acceptable, the reasons which caused the error are still discussed here. The quantization level of the Hough space will affect the accuracy of straight line parameters, and hence the fitting lines will slightly deviate from the ideal position. The integer pixel level is used in the center estimation based on the maximum probability criterion. The true value from the manual measurement may be not very accurate. Additionally, when the meter image with low spatial resolution is applied in the calculations, the shorter scale lines may affect the fitting accuracy. As a result, these factors will lead to errors of location.

5. Conclusions

A method based on machine vision is proposed in the paper to detect pointer features including the rotation center of pointer, the pointer centerline and the pointer direction. The new method is based on implementation of centripetalism of annular scale lines to detection, and so it is a structural feature based method that is different to the traditional region-based methods. The simulation examples and experiments prove that the proposed method can effectively overcome the problem of the optical axis of camera not being perpendicular to the meter surface. It is also not sensitive to uneven light illumination. These advantages indicate that the proposed method has strong robustness and can be applied in many complex situations to detect pointer features. This will be also very useful in automatic reading recognition in the next step.

In the current work, only longer scale lines are used in the rotation center estimation. In practice, the more scales lines can also be used and the reliability of the method will further improve. In future work, we intend to complete our method to determine the reading value of meter and further improve the adaptability of the method to more complex industry environments.

Acknowledgements

This work was supported by the National Natural Science Foundation of China (51765054), the Natural Science Foundation of Inner Mongolia of China (2020LH06002) and the Science Foundation of the Inner Mongolia University of Technology of China (X201703 and ZZ201902).

References

[1] Alegria, E. C., & Serra, A. C. (2000). Automatic calibration of analog and digital measuring instruments using computer vision. *IEEE Transactions on Instrumentation and Measurement, 49*(1), 94–99. https://doi.org/10.1109/19.83631710.1109/19.836317.

[2] Zheng, C., Wang, S., Zhang, Y., Zhang, P., & Zhao, Y. (2016). A robust and automatic recognition system of analog instruments in power system by using computer vision. *Measurement, 92*, 413–420. https://doi.org/10.1016/j.measurement.2016.06.045

[3] Galliana, F., & Lanzillotti, M. (2019). Evaluation of a high-precision digital multimeter by the laboratory of calibration of multifunction electrical instruments of INRIM. *Metrology and Measurement Systems, 26*(2). 283–296. https://doi.org/10.24425/mms.2019.128356

[4] Hemming, B., Fagerlund, A., & Lassila, A. (2007). High-accuracy automatic machine vision based calibration of micrometers. *Measurement Science and Technology, 18*(5), 1655–1660. https://doi.org/10.1088/0957-0233/18/5/058

[5] Gao, J. W., Xie, H. T., Zuo, L., & Zhang, C. H. (2017). A robust pointer meter reading recognition method for substation inspection robot. *2017 International Conference on Robotics and Automation Sciences (ICRAS)*, China, 43–47. https://doi.org/10.1109/ICRAS.2017.8071914

[6] Yifan, M., Qi, J., Junjie, W., & Guohui, T. (2017, October). An automatic reading method of pointer instruments. *2017 Chinese Automation Congress (CAC)*, China, 1448–1453. https://doi.org/10.1109/CAC.2017.8242995

[7] Belan, P. A., Araujo, S. A., & Librantz, A. F. H. (2013). Segmentation-free approaches of computer vision for automatic calibration of digital and analog instruments. *Measurement, 46*(1), 177–184. https://doi.org/10.1016/j.measurement.2012.06.005

[8] Yang, Z., Niu, W., Peng, X., Gao, Y., Qiao, Y., & Dai, Y. (2014, April). An image-based intelligent system for pointer instrument reading. *2014 4th IEEE International Conference on Information Science and Technology*, China, 780–783. https://doi.org/10.1109/ICIST.2014.6920593

[9] Song, W., Zhang, W. J., Zhang, J., Wang, Y., Zhou, Q., & Shi, W. (2014). Meter reading recognition method via the pointer region feature. *Chinese Journal of Scientific Instrument, S2*, 50–58. (in Chinese) http://www.cnki.com.cn/Article/CJFDTotal-YQXB2014S2008.htm

[10] Zhang, W. J., Xiong, Q. Y., Zhang, J. Q., Wang, Y., Jiang, P., & Wang, C. (2015). Pointer type meter reading recognition based on visual saliency. *Journal of Computer-Aided Design & Computer Graphics, 27*(12), 2282–2295. (in Chinese) http://www.cnki.com.cn/Article/CJFDTotal-JSJF201512006.htm

[11] Chi, J., Liu, L., Liu, J., Jiang, Z., & Zhang, G. (2015). Machine vision based automatic detection method of indicating values of a pointer gauge. *Mathematical Problems in Engineering*. https://doi.org/10.1155/2015/283629

[12] Ma, Y., & Jiang, Q. (2018). A robust and high-precision automatic reading algorithm of pointer meters based on machine vision. *Measurement Science and Technology*, 30(1), 015401. https://doi.org/10.1088/1361-6501/aaed0a

[13] Hengqiang, S., & Changji, W. (2012). A new algorithm based on super-green features for ostu's method using image segmentation. *World Automation Congress 2012*, Mexico. https://ieeexplore.ieee.org/document/6321876

[14] Heyduk, A. (2019). Elliptical shape and size approximation of a particle contour. *Proceedings of IOP Conference Series: Earth and Environmental Science*, Poland, *261*(1). https://doi.org/10.1088/1755-1315/261/1/012013

[15] Yam-Uicab, R., López-Martínez, J., Llanes-Castro, E., Narvaez-Díaz, L., & Trejo-Sánchez, J. (2018). A parallel algorithm for the counting of ellipses present in conglomerates using GPU. *Mathematical Problems in Engineering, 2018*. https://doi.org/10.1155/2018/5714638

Metrol. Meas. Syst., Vol. 27 (2020), No. 4, pp. 589–599
DOI: 10.24425/mms.2020.134840

[16] Goh, T. Y., Basah, S. N., Yazid, H., Safar, M. J. A., & Saad, F. S. A. (2018). Performance analysis of image thresholding: Otsu technique. *Measurement, 114*, 298–307. https://doi.org/10.1016/j.measurement.2017.09.052

[17] Xu, Z., Shin, B. S., & Klette, R. (2015). Closed form line-segment extraction using the Hough transform. *Pattern Recognition, 48*(12), 4012–4023. https://doi.org/10.1016/j.patcog.2015.06.008

[18] Li, D., Chen, H., Sheng, Y., & Yang, L. (2019). Dual-station intelligent welding robot system based on CCD. *Measurement Science and Technology, 30*(4), 045401. https://doi.org/10.1088/1361-6501/ab02d7

[19] Fatan, M., Daliri, M. R., & Shahri, A. M. (2016). Underwater cable detection in the images using edge classification based on texture information. *Measurement, 91*, 309–317. https://doi.org/10.1016/j.measurement.2016.05.030

Fu-Zhong Bai received his Bachelor's and Master's degrees from Inner Mongolia University of Technology in 2001 and 2004, and his doctor's degree from University of Chinese Academy of Sciences in 2010. He is currently a professor of the Inner Mongolia University of Technology. His current research interests include structural light 3D measurement, visual detection and laser interferometry.

Hai-Bo Zhuo was born in Inner Mongolia, China in 1988. He received the M.Sc.(2020) degree from the Inner Mongolia University of Technology (IMUT), China. His research interests include digital image processing and robot control technology.

Yong-Xiang Xu obtained the B.Sc. and M.Sc. degree in Mechatronic engineering from the Inner Mongolia University of Technology, Hohhot, China, in 1997, and 2007, respectively. He is currently Assistant Professor with the Inner Mongolia University of Technology, China. His research activity focuses on measurement technology and instrument, and visual detection and image processing.